Journal of Applied Polymer Science

Synthesis, Characterization, and Properties of Acrylate-Modified Tung-Oil Waterborne Insulation Varnish

Qing Ge,[1] Hualin Wang,[1,2] Yi She,[1] Suwei Jiang,[1] Mengye Cao,[1] Linfeng Zhai,[1] Shaotong Jiang[2,3]

[1]School of Chemistry and Chemical Technology, Hefei University of Technology, Hefei Anhui 230009, People's Republic of China
[2]Anhui Institute of Agro-Products Intensive Processing Technology, Hefei Anhui 230009, People's Republic of China
[3]School of Biotechnology and Food Engineering, Hefei University of Technology, Hefei, Anhui 230009, People's Republic of China
Correspondence to: H. Wang (E-mail: hlwang@hfut.edu.cn)

ABSTRACT: An acrylate-modified tung-oil waterborne insulation varnish was synthesized from tung oil, maleic anhydride, and acrylates via a Diels–Alder reaction and free-radical polymerization, and the varnish could be solidified at a relatively low temperature with blocked hexamethylene diisocyanate as a curing agent. The resulting films were characterized by Fourier transform infrared spectroscopy, thermogravimetric analysis, and differential scanning calorimetry. The insulation properties (electrical insulation strength, volume resistivity, and surface resistivity) of the varnish films were tested, and the resistances of films to salted water were evaluated. With an increase in the maleic anhydride content, the thermal stability of the film was improved, whereas the electrical insulation strength, volume resistivity, and surface resistivity decreased. The electrical insulation strength of the film after it was immersed in the NaCl solution was lower than that in dry state, and it decreased as the immersed time was prolonged. In particular, the electrical insulation strength loss of the film increased significantly at maleic anhydride contents beyond 25 wt %. Furthermore, the hardness of the film increased with increasing methyl methacrylate/*N*-butyl acrylate ratio, whereas the flexibility and adhesion of film decreased to a certain degree at the same time. © 2014 Wiley Periodicals, Inc. J. Appl. Polym. Sci. **2015**, *132*, 41608.

KEYWORDS: biopolymers and renewable polymers; coatings; properties and characterization; resins

Received 31 July 2014; accepted 7 October 2014
DOI: 10.1002/app.41608

INTRODUCTION

In recent years, growing attention has been paid to new polymeric materials from seed oils because of the availability, low cost, and renewability of these oils.[1,2] Tung oil, a Chinese wood oil, is a major product from the seeds of tung trees.[3,4] It is an important industrial raw material, and Chinese tung-oil production accounted for 80% of world production.[5] The major component of tung oil is a glyceride composed of α-eleostearic acid (*cis*−9, *trans*−11, *trans*−13-octadecatrienoic acid).[6] Tung oil has been widely used in the preparation of varnishes,[7] paints,[8] and related materials because of its highly unsaturated and conjugated triene system.[9–11] Compared to other unconjugated drying oils, such as soybean and linseed oils, tung oil has a faster drying time, a better water resistance, and higher hardness.[12] Furthermore, it can be chemically modified more easily to obtain the desired performance; this contributes to its conjugated structure. It is well known that tung-oil fatty acids can undergo a Diels–Alder reaction easily with a dienophile because of the conjugated double bonds.[13] The Diels–Alder reaction has been successfully used to synthesize tung-oil alkyds[12] and styrene–tung-oil resins.[14] Several researchers have modified tung oil to prepare desired polymer materials via thermal, free-radical and even cationic polymerization.[15,16]

Acrylates are widely used as a principal raw material for functional materials,[17,18] and different acrylic monomers provide distinct properties for the final products. Methyl methacrylate (MMA) and methyl acrylate (MA) afford hardness, exterior durability, and water resistance.[19] *N*-Butyl acrylate (BA) and ethyl acrylate improve the flexibility and film-forming properties of polymers.[20] The grafting of acrylic macroradicals may take place via two ways: by addition to the double bonds of the fatty acid chain in alkyd resins or by abstraction of alkyd resin allylic hydrogens[21] A new type of acrylated alkyd grafting acrylic copolymer, prepared via radical polymerization to the unsaturated sites located in the backbone and the fatty acid chains, was reported.[22] Some researchers have reported the investigation of acrylic-resin-modified vegetable oils;[18,23,24] however, we found no research on the investigation of acrylate-modified tung-oil waterborne insulation varnishes.

In this study, an acrylate-modified tung-oil waterborne insulation varnish was prepared from tung oil, maleic anhydride, and acrylates via a Diels–Alder reaction and free-radical

polymerization, and the structures of the resulting varnish films were characterized. The influence of the maleic anhydride content on the thermal stability, insulation properties, and resistance to salted water was emphasized. Furthermore, the effects of the MMA/BA ratio on the mechanical properties of the films were investigated.

EXPERIMENTAL

Materials

Tung oil was obtained from Jiangsu Donghu Bio-Energy Plant Plantation (China). Maleic anhydride, *N,N*-dimethyl ethanolamine, hexamethylene diisocyanate (HDI), and methylethylketoxime (MEKO) were purchased from Shanghai Lingfeng Chemical Reagent Co., Ltd.(Shanghai, China). BA, MMA, hydroxypropyl acrylate (HPA), isopropyl alcohol, and 1-methoxy-2-propanol were purchased from Sinopharm Chemical Reagent Co., Ltd. (Shanghai, China). The initiator 2-methylpropionitrile was obtained from Aldrich Chemical Co. (Milwaukee, WI). All of the chemical reagents used were analytical grade.

Synthesis of Acrylate-Modified Tung-Oil Resin

The synthesis of acrylate-modified tung-oil resin was performed in a 250-mL, three-necked, round-bottomed flask equipped with a nitrogen (N_2) gas inlet, reflux condenser, and mechanical agitator in an oil bath. At first, 30 g of tung oil and the required maleic anhydride (all on the basis of the weight of tung oil) were added to the flask, and then, the mixture was heated up to 120–125°C and reacted for 1 h to give a yellow transparent tung oil–MA adduct. Second, 15 g of isopropyl alcohol was added to the flask when the temperature cooled to 83°C. Subsequently, 15.83 g of MMA and BA, 4.89 g of HPA, and 0.1658 g of 2-methylpropionitrile were added by dropwise within 30 min. On the basis of our experimental data, the ratio of MMA/BA used was 3:1 in most experiments. Two hours later, the system was cooled to room temperature, and 5 g of isopropyl alcohol and 10 g 1-methoxy-2-propanol were added. Meanwhile, the pH value of the system was adjusted to 8.0–8.5 by *N,N*-dimethyl ethanolamine. Finally, the curing-agent-blocked HDI was added to the system with stirring for 0.5 h to give a pale yellow transparent acrylate-modified tung-oil resin. To obtain the blocked HDI, 3.20 g of HDI was blocked by 3.64 g of MEKO at 80°C for 4 h beforehand.

Curing of Acrylate-Modified Tung-Oil Resin

A square copper sheet (4.0 cm ×7.5 cm × 0.1 mm) polished with 800-grit emery paper was used as a substrate. The as-prepared acrylate-modified tung-oil resin was diluted by equal amount deionized water, and then, the coating on the copper sheet was prepared by the immersion method and cured in the oven at 125°C for 2 h.

Measurement and Characterization

Structure and Thermodynamic Analysis. The structures of the cured films were characterized by Fourier transform infrared spectroscopy (FTIR); this was completed with a Nicolet 6700 spectrometer (Thermo Nicolet) with KBr pellets. The thermal stability was assessed with a TGA 209 thermogravimetric analyzer (Netzsch, Germany). The samples were heated up to 800°C at a constant heating rate of 10°C/min under a nitrogen flow at rate of 50 mL/min. Differential scanning calorimetry (DSC) was conducted by a Mettler Toledo DSC-851e (Im Langacher, Switzerland) under a nitrogen atmosphere at a flow of 20 mL/min.

Water Absorption Testing. The weighed dried samples were immersed in a bath with deionized water at 25°C for 24 h, and then, the samples were removed from distilled water and weighed. The water absorption of the film was calculated as follows:

$$\text{Water absorption} = \frac{m_2 - m_1}{m_1 - m_0} \times 100\% \quad (1)$$

where m_o is the weight of the copper sheet, m_1 is the weight of the dried sample, and m_2 is the weight of the sample with the absorbed water.

Insulation Properties. The electrical insulation strength was measured with a Quadtech Guardian 20 kV HiPot tester (Marlborough, MA). An electrostatic sandwich setup was used for all breakdown measurements, and two aluminum metalized biaxially oriented polypropylene film were used as flexible electrodes. The voltage was increased until the electric breakdown and all measurements were conducted at 25°C in air. The breakdown data were recorded when the breakdown site was in the center area of the masked film. The dry- and wet-state films were measured. The electrical insulation strength (E) was determined as follows:

$$E = \frac{V}{d} \quad (2)$$

where the V is breakdown voltage and d is the thickness of the film (cm).

The volume and surface resistivities were measured with a high resistivity meter (model ZC-36, Shanghai Sixth Meter Co., Ltd.). The two surfaces connected to the electrodes were first treated with colloidal silver paint to remove the top surface layers, which were rich in polymer, and to ensure good contact between the sample surface and the electrodes. The volume resistivity (ρ_v) was calculated as follows:

$$\rho_v = R_V \frac{A}{d} \quad (3)$$

where R_V is the volume resistance (Ω) and A is the area of the sample contacting the electrode (cm^2). The surface resistivity (ρ_s) was calculated as follows:

$$\rho_s = R_X \frac{P}{g} \quad (4)$$

where R_X is the surface resistance (Ω), P is the effective perimeter of the guarded electrode (cm), and g is the distance between the electrodes (cm).

Salted Water Resistance Testing. The specimen was immersed in a 3.5% NaCl solution at 25°C for a certain period, and then, the surface of the specimen was observed with scanning electron microscopy (SEM; SU8020, Hitachi, Japan), and all of the specimens were sputter-coated with a layer of gold. To evaluate the effect of the salt solution, the electrical insulation strength of

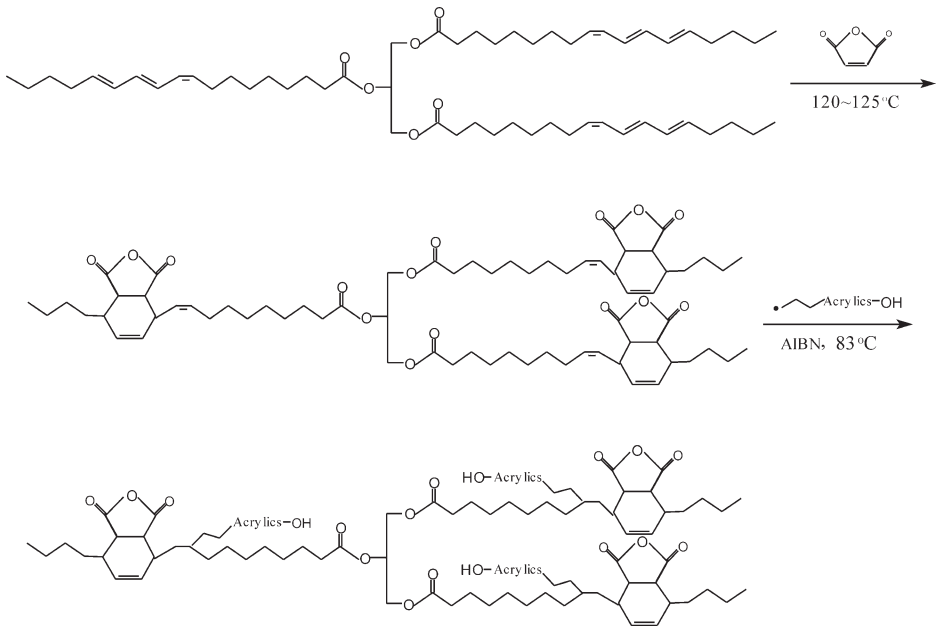

Scheme 1. Synthetic route and theoretical structure of the tung oil–MA adduct and the grafting mechanism of the acrylate–tung oil.

the specimen was tested after it was immersed in a salt solution for 24 and 168 h.

Mechanical Properties. Films on copper sheets were used to test the crosshatch adhesion (ASTM D 3359), pencil hardness (ASTM D 3363), and conical mandrel flexibility (ASTM D 522).

RESULTS AND DISCUSSION

Principles

Tung oil was reacted with maleic anhydride via a Diels–Alder reaction to produce a tung oil–MA adduct; subsequently, the tung oil–MA adduct was reacted with acrylic monomers via a free-radical reaction (Scheme 1). HDI blocked by MEKO was used as a curing agent. Upon heating, the weak bond of the blocked HDI broke and regenerated isocyanate groups; these could react with the —OH groups derived from HPA in the desired manner to form more thermally stable bonds.[25] The overall reaction is depicted in Scheme 2, where BH represents the blocking agent.

Structure and Deblocking Temperature of the Curing Agent

Figure 1 illustrates the FTIR spectra of the HDI and HDI blocked by MEKO. As shown in Figure 1(a), the strong characteristic absorption peak at 2275 cm^{-1} was assigned to the stretching vibrations of —NCO in HDI.[26] When HDI was blocked by MEKO at 80°C for 2 h, the intensity of —NCO was weakened because of the blocking reaction [Figure 1(b)]. Four hours later, the characteristic absorption peaks of —NCO disappeared completely, and the characteristic absorption peaks of —NH at 3369 and 1718 cm^{-1} were present [Figure 1(c)]. This implied that the —NCO groups in HDI were blocked entirely at 80°C for 4 h.

The deblocking temperature of the blocked HDI played an important role in film curing. DSC was conveniently used to

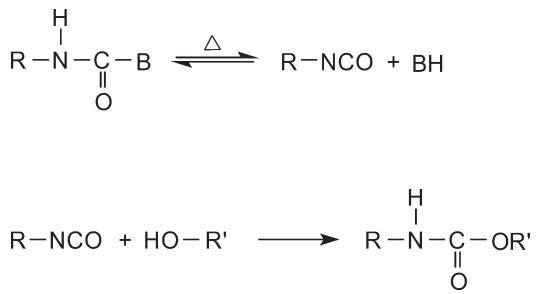

Scheme 2. Blocking and deblocking mechanism of isocyanate.

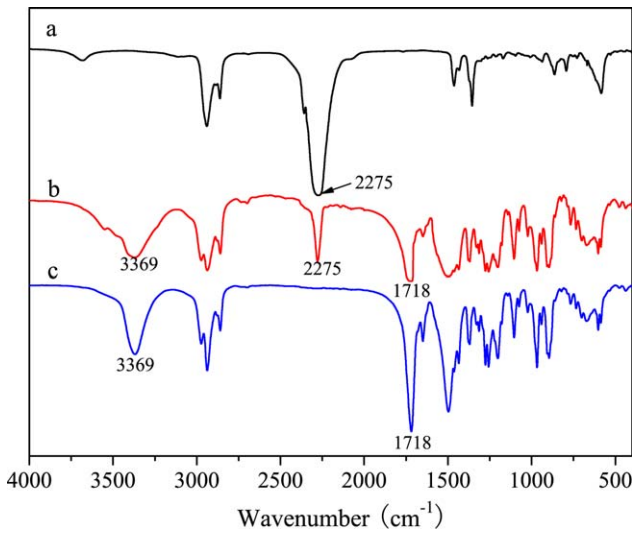

Figure 1. FTIR spectra of the samples: (a) HDI, (b) HDI blocked by MEKO for 2 h, and (c) HDI blocked by MEKO for 4 h. [Color figure can be viewed in the online issue, which is available at wileyonlinelibrary.com.]

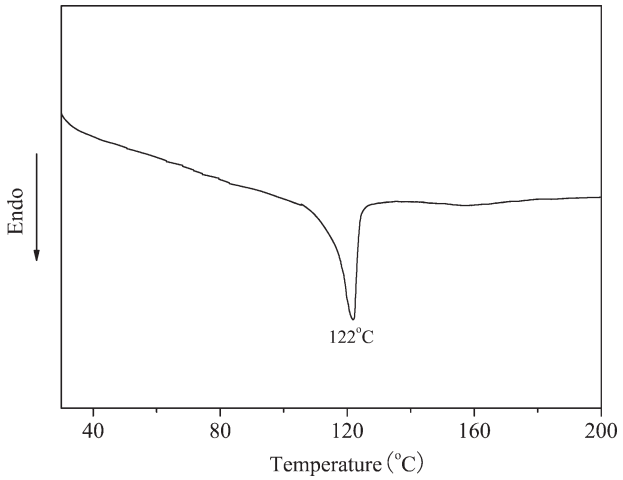

Figure 2. DSC curve of the HDI blocked by MEKO for 4 h.

investigate the deblocking temperature of the blocked HDI. The presence of an endothermic peak in the DSC thermographs of the blocked isocyanate was assigned to the deblocking reaction and the evaporation of the blocking agent.[27] Figure 2 shows the DSC curve of the blocked HDI. As shown in Figure 2, the onset temperature of the deblocking reaction was about 104°C, and the maximum temperature of the deblocking reaction was about 122°C. On the basis of the experimental data, the curing temperature for the acrylate-modified tung-oil resin was set at 125°C.

Characterization of the Acrylate-Modified Tung-Oil Films

Figure 3 illustrates the FTIR spectra of tung oil and acrylate-modified tung-oil film, respectively. In the spectrum of tung oil [Figure 3(a)], several characteristic peaks of tung oil were observed. Three absorption peaks at 3014, 991, and 964 cm^{-1} were attributed to the tung oil's conjugated triene structure.[9] Two absorption peaks at 2925 and 2854 cm^{-1} were assigned to the stretching vibration of $-CH_3$ and $-CH_2-$, whereas the strong absorption peaks at 1745 cm^{-1} were ascribed to the stretching vibration of C=O in the ester group. Compared with Figure 3(a), the characteristic absorption of the tung oil conjugated triene at 3014, 991, and 964 cm^{-1} disappeared in the spectrum of the acrylate-modified tung-oil film [Figure 3(b)]. These disappearance bands showed that the conjugated triene on tung-oil molecules had reacted with the unsaturated double bonds on maleic anhydride through a Diels–Alder reaction. Furthermore, the bond at 844 cm^{-1} in Figure 3(b) was a characteristic peak of polyacrylate; this indicated that the acrylate reacted with the double bonds on tung oil (Scheme 1).

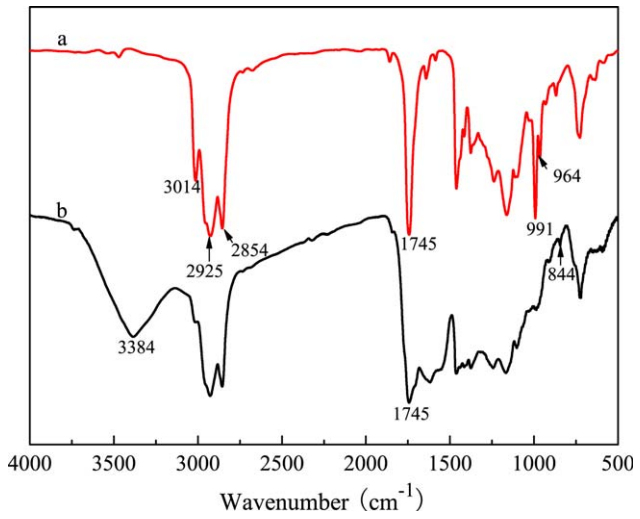

Figure 3. FTIR spectra of the samples: (a) tung oil and (b) acrylate-modified tung oil film. [Color figure can be viewed in the online issue, which is available at wileyonlinelibrary.com.]

Thermal Stability of the Films

Thermogravimetric Analysis (TGA) and Derivative Thermogravimetric (DTG) Analyses. Thermal stability is important for the film of insulating varnish, and the TGA curves of the films with different maleic anhydride contents are shown in Figure 4(A). As shown in Figure 4(A), three-stage thermal

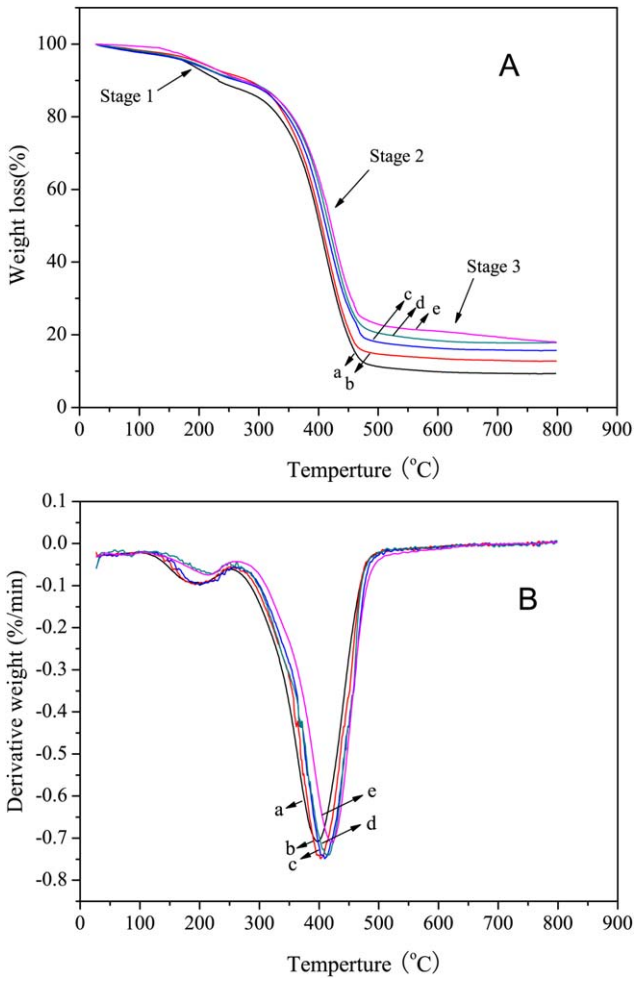

Figure 4. (A) TGA curves of the samples with maleic anhydride contents of (a) 15, (b) 20, (c) 25, (d) 30, and (e) 35 wt % (MMA/BA ratio = 3:1). (B) DTG curves of the samples with maleic anhydride content of (a) 15, (b) 20, (c) 25, (d) 30, and (e) 35 wt % (MMA/BA ratio = 3:1). [Color figure can be viewed in the online issue, which is available at wileyonlinelibrary.com.]

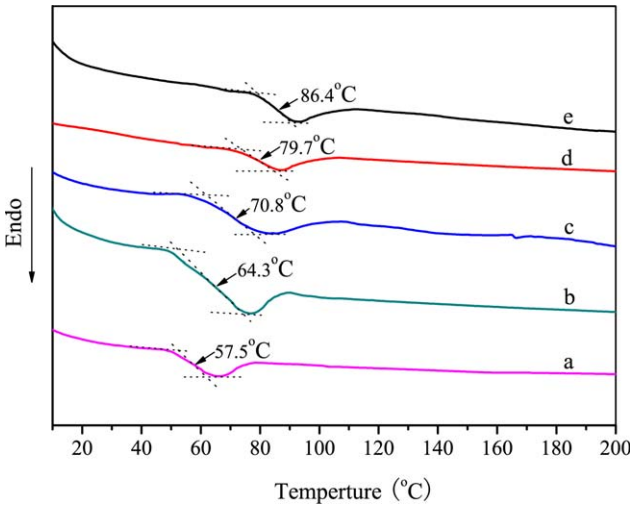

Figure 5. DSC curves of the samples with maleic anhydride contents of (a) 15, (b) 20, (c) 25, (d) 30, and (e) 35 wt % (MMA/BA ratio = 3:1). [Color figure can be viewed in the online issue, which is available at wileyonlinelibrary.com.]

degradation was present in each curve. The weight loss in the first stage was mainly attributed to the evaporation of the high-boiling solvent remaining in the film, and the release of the blocking agent in the deblocking reaction of the blocked HDI. The severe weight loss present in the second stage was due to the cleavages of the C—O and C—C linkages. The last stage corresponded to the gradual degradation of the char residue. The temperature at 50% weight loss[28] was used to evaluate the thermal stability of the polymeric system. Figure 4(A) shows that the temperature at 50% weight loss increased from 402 to 421°C as the maleic anhydride content increased from 15 to 35 wt %. On the basis of TGA, the corresponding DTG analysis of the film is shown in Figure 4(B). It was clear that the maximum weight loss rates of the films with maleic anhydride contents of 15, 20, 25, 30, and 35 wt % were about 402, 405, 412, 417, and 421°C, respectively. Combined with the thermogravimetric and DTG results, the thermal stability of the film was improved with the incorporation of maleic anhydride. The reason was that the Diels–Alder reaction occurred between tung oil and maleic anhydride and formed a stable six-membered ring. As the maleic anhydride content increased below the stoichiometric ratio (maleic anhydride to tung oil = 3:1 mol/mol), the number of six-membered rings in the polymeric matrix increased and improved the thermal stability of the films.

DSC Analysis. To investigate the effect of the maleic anhydride content on the thermal stability, DSC was used to study the glass-transition temperature (T_g) of the films, and the results are shown Figure 5. As shown in Figure 5, the films with contents of maleic anhydride of 15, 20, 25, 30, and 35 wt % showed T_g's of about 57.5, 64.3, 70.8, 79.7, and 86.4°C, respectively. There was an endothermic peak near the glass transition in each curve because of the enthalpy relaxation. Enthalpy relaxation phenomena are often observed in the region of T_g during the heating of glassy materials.[29] According to the DSC curves, the T_g values of the films increased with increasing maleic anhydride content; this indicated that the incorporation of maleic anhydride had a positive effect on the glass transition of the polymer. As the content of the six-membered ring in the polymer increased with increasing maleic anhydride content, the rigidity of the polymer chain was improved, and it limited the movement of the polymer segments and resulted in an increase in T_g accordingly.[30]

Water Absorption

The variation of the water absorption of the films with different contents of maleic anhydride is illustrated in Figure 6. As the curve shows, the water absorption of the films increased with increasing maleic anhydride content from 15 to 35 wt %. Under the same reaction mechanism and dosage of acrylic monomers, a higher maleic anhydride content produced more carboxyl groups, and this increased the water absorption capability of the films. Excessive water absorption of the film had an adverse effect on the properties of the film.

Insulation Properties of the Films

Electrical Insulation Strength. The electrical insulation strength of the film is the most significant factor in the evaluation of the properties of resin insulation varnishes. The electrical insulation strengths of the films in the dry and wet state are depicted in Figure 7. As the content of maleic anhydride increased, the electrical insulation strength of the films showed a declining trend, under both the dry and wet states. The reason was that the number of carboxyl groups in the polymeric matrix increased with the addition of maleic anhydride. As the carboxyl groups were polar, the conductivity of the films increased with the incorporation of carboxyl groups; as a result, the films' insulation performance decreased.[31] Compared with that of the film in the dry state, the electrical insulation strength in the wet state was lower at each given maleic anhydride content because of the absorbed water.

Volume Resistivity and Surface Resistivity. The volume resistivity and surface resistivity are also important factors for

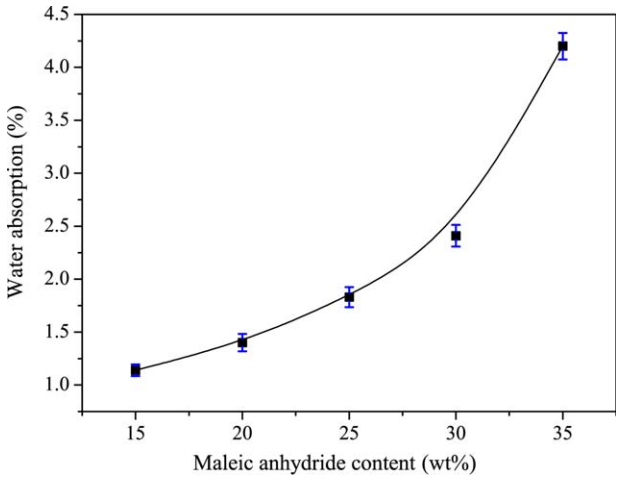

Figure 6. Water absorption of the films (MMA/BA ratio at 3:1). [Color figure can be viewed in the online issue, which is available at wileyonlinelibrary.com.]

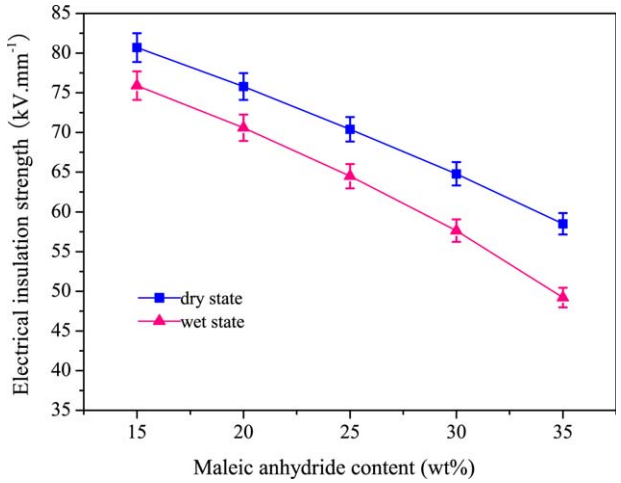

Figure 7. Electrical insulation strength of the films (25°C, MMA/BA ratio = 3:1). [Color figure can be viewed in the online issue, which is available at wileyonlinelibrary.com.]

evaluating the material's insulation properties. The volume resistivity and surface resistivity of the films with different maleic anhydride contents in the dry and wet states are shown in Figures 8(A,B). As shown in Figure 8(A), the volume resistivity of the films decreased with increasing maleic anhydride content in both the dry and wet states, and the value of the volume resistivity of the films in the dry state at each given maleic anhydride content was higher than that in the wet state. Similar results were observed in the surface resistivity of the films [Figure 8(B)]. As previously mentioned, the increase in the maleic anhydride content caused an increase in the number of polar carboxyl groups in the polymeric matrix. As a result, the volume resistivity and surface resistivity of the films decreased correspondingly. Moreover, as the films absorbed water, their conductivity increased and caused a decrease in the volume resistivity and surface resistivity of the film at each given maleic anhydride content.

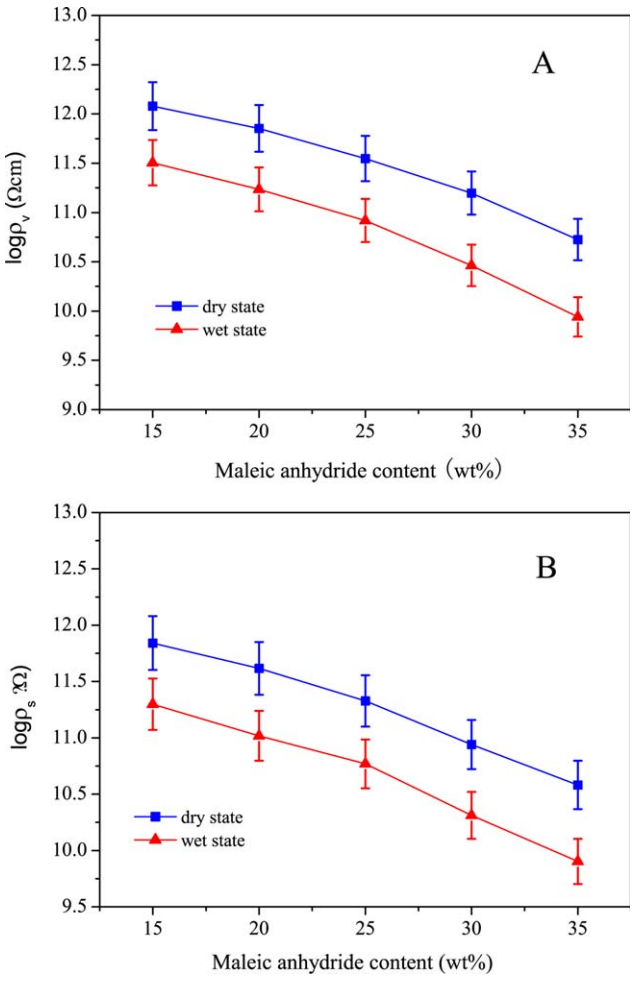

Figure 8. (A) Volume resistivity of the films. (B) Surface resistivity of the films (25°C, MMA/BA ratio = 3:1). [Color figure can be viewed in the online issue, which is available at wileyonlinelibrary.com.]

Salted Water Resistance Testing

To investigate the resistance to salted water as a function of the maleic anhydride content, the films were immersed in 3.5 wt % NaCl solutions, and the results are shown in Figure 9(A). On the basis of Figure 9(A), the electrical insulation strength loss of

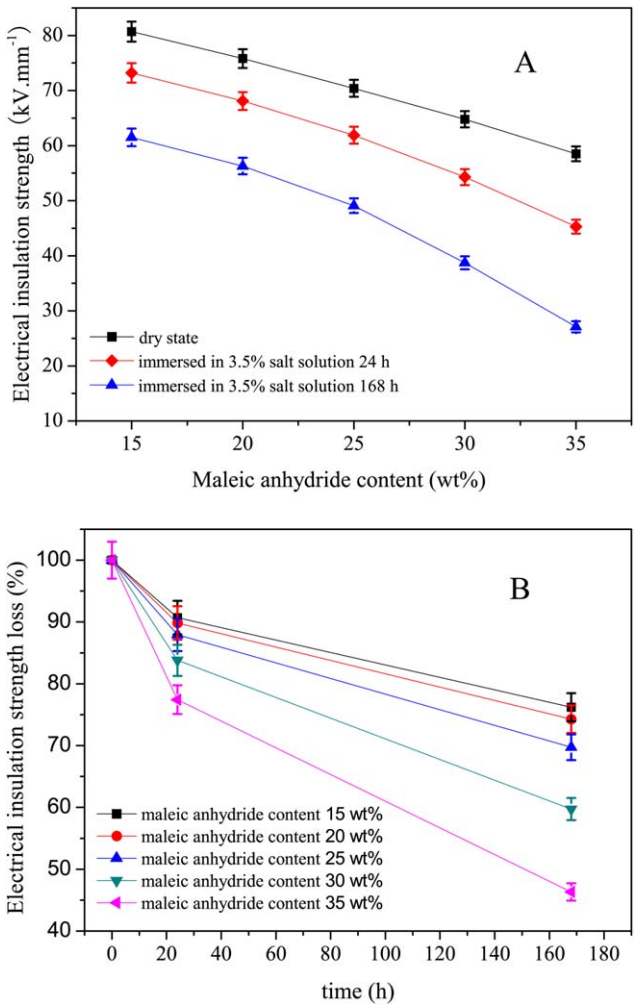

Figure 9. (A) Electrical insulation strength of the films. (B) Electrical insulation strength loss of the films (immersed in a 3.5% NaCl solution at 25°C, MMA/BA ratio = 3:1). [Color figure can be viewed in the online issue, which is available at wileyonlinelibrary.com.]

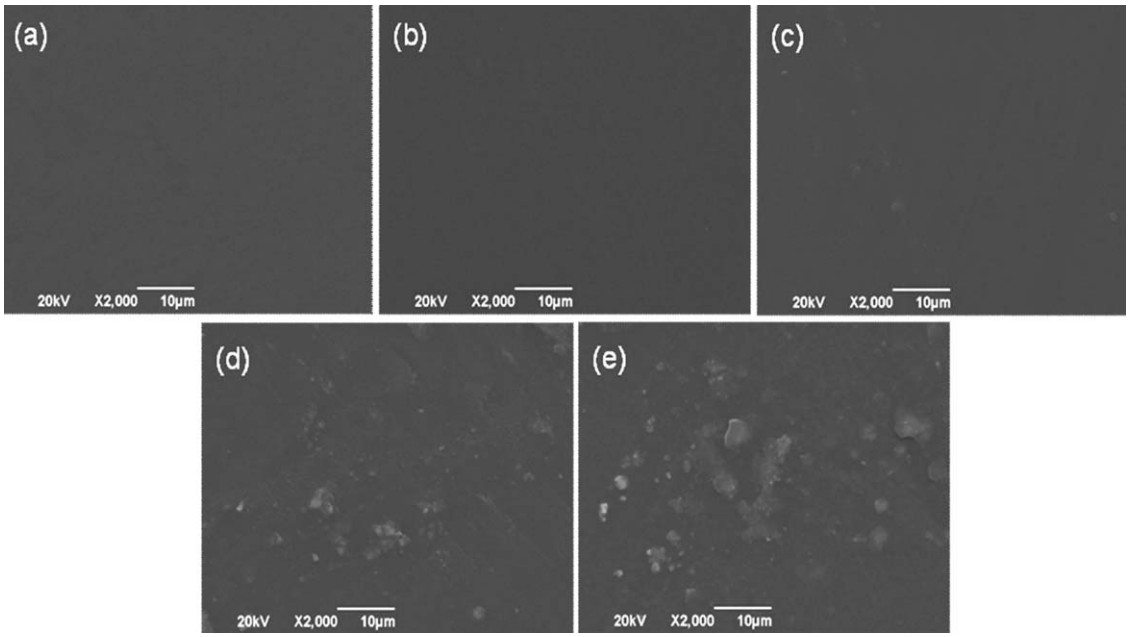

Figure 10. SEM photographs of the film surfaces with maleic anhydride contents of (a) 15, (b) 20, (c) 25, (d) 30, and (e) 35 wt % (immersed in an NaCl solution at 25°C for 168 h, MMA/BA ratio = 3:1).

each film is illustrated in Figure 9(B). A similar downtrend was observed for the films in the dry state and after they were immersed in an NaCl solution [Figure 9(A)]. As expected, the electrical insulation strength of the films after immersion in the NaCl solution was lower than that in the dry state, and it decreased as the immersed time prolonged. Notably, the electrical insulation strength loss of film increased significantly at maleic anhydride content beyond 25 wt % [Figure 9(B)]. Correspondingly, the film surfaces with maleic anhydride contents of 15, 20, and 25 wt % were smooth, and no obvious blisters were present, whereas when the maleic anhydride content reached 30 wt % and above, lots of blisters were present [Figure 10]. Because the polar carboxyl groups in the polymeric matrix derived from maleic anhydride improved the hydrophilicity of the films and Na^+ or Cl^- might have diffused into the polymeric matrix, the electrical insulation strength decreased after immersion in an NaCl solution. In particular, the sharp decrease in the electrical insulation strength was present for maleic anhydride contents of 30 wt % and above.

Effect of the MMA/BA Ratio on the Film Mechanical Properties

As it is known, MMA provides exterior durability and hardness, and BA adds flexibility and exterior durability.[32] In this study, MMA was used as a hard monomer, and BA was used as a soft monomer. To investigate the effect of the MMA/BA ratio on the film mechanical properties, including the hardness, flexibility, and adhesion. The MMA/BA ratio used were 1:1, 2:1, 3:1, and 4:1 (mol/mol), and the maleic anhydride content was set at 25 wt %. The effects of the MMA/BA ratio on the film properties are presented in Table I. According to Table I, the hardness of the film increased with increasing MMA/BA ratio; meanwhile, the flexibility and adhesion of the film decreased to a certain degree. The reason was that the addition of MMA enhanced the rigidity of the molecular segment; on the contrary, BA contributed to the flexibility. Moreover, the excessive MMA increased the cohesion of the molecular segment and caused a decrease in the adhesion of the film.

CONCLUSIONS

An acrylate-modified tung-oil waterborne insulation varnish was successfully synthesized via a Diels–Alder reaction and free-radical polymerization, and the varnish was solidified at 125°C with blocked HDI as a curing agent. As the maleic anhydride content increased, the thermal stability of the film improved, and the electrical insulation strength, volume resistivity, and surface resistivity decreased. The electrical insulation strength of the film after immersion in the NaCl solution was lower than that in the dry state, and it decreased as the immersion time was prolonged. In particular, the electrical insulation strength loss of the films increased significantly at maleic anhydride contents beyond 25 wt %. Moreover, the hardness of the films increased with increasing MMA/BA ratio, whereas the flexibility and adhesion of the films decreased to a certain degree. The electrical insulation strength, volume resistivity, and surface

Table I. Effect of the MMA/BA Ratio on the Film Mechanical Properties

MMA/BA ratio (mol/mol)	Dry film thickness (μm)	Pencil hardness	Conical mandrel flexibility diameter (in.)	Crosshatch adhesion
1:1	48.3	2H	1/8	5B
2:1	50.0	2H	1/8	5B
3:1	51.7	3H	1/8	4B
4:1	53.3	4H	1/4	2B

resistivity of the resulting films were not less than 70.4 kV/mm, 3.53×10^{11} Ω cm, and 2.09×10^{11} Ω, respectively, at a maleic anhydride content below 25 wt %, respectively; these films may have potential as an effective immersion insulation varnish for the spindle of electric motor.

REFERENCES

1. Biermann, U.; Bornscheuer, U.; Meier, M. A.; Metzger, J. O.; Schäfer, H. *J. Angew. Chem. Int. Ed.* **2011**, *50*, 3854.
2. Xia, Y.; Quirino, R. L.; Larock, R. C. *J. Renew. Mater.* **2013**, *1*, 3.
3. Li, F.; Larock, R. C. *J. Appl. Polym. Sci.* **2000**, *78*, 1044.
4. Mosiewicki, M.; Casado, U.; Marcovich, N.; Aranguren, M. *Polym. Eng. Sci.* **2009**, *49*, 685.
5. Zhong, C.; Cao, Y. X.; Li, B. Z.; Yuan, Y. *J. Biofuel. Bioprod. Biorefining* **2010**, *4*, 326.
6. Li, F.; Larock, R. C. *Biomacromolecules* **2003**, *4*, 1018.
7. Thanamongkollit, N.; Miller, K. R.; Soucek, M. D. *Prog. Org. Coat.* **2012**, *73*, 425.
8. Samadzadeh, M.; Boura, S. H.; Peikari, M.; Ashrafi, A.; Kasiriha, M. *Prog. Org. Coat.* **2011**, *70*, 383.
9. Liu, C.; Yang, X.; Cui, J.; Zhou, Y.; Hu, L.; Zhang, M.; Liu, H. *Bioresources* **2011**, *7*, 447.
10. Das, K.; Ray, D.; Banerjee, C.; Bandyopadhyay, N.; Mohanty, A. K.; Misra, M. *J. Appl. Polym. Sci.* **2011**, *119*, 2174.
11. Xia, Y.; Larock, R. C. *Green Chem.* **2010**, *12*, 1893.
12. Thanamongkollit, N.; Soucek, M. D. *Prog. Org. Coat.* **2012**, *73*, 382.
13. Trumbo, D.; Mote, B. *J. Appl. Polym. Sci.* **2001**, *80*, 2369.
14. Brunner, H.; Tucker, D. *J. Appl. Chem.* **1951**, *1*, 563.
15. Park, S.-J.; Jin, F.-L.; Lee, J.-R. *Mater. Sci. Eng. A* **2004**, *374*, 109.
16. Huang, Y.; Pang, L.; Wang, H.; Zhong, R.; Zeng, Z.; Yang, J. *Prog. Org. Coat.* **2013**, *76*, 654.
17. Matsuura, Y.; Onda, A.; Ogo, S.; Yanagisawa, K. *Catal. Today* **2014**, *226*, 192.
18. Dziczkowski, J.; Soucek, M. D. *Prog. Org. Coat.* **2012**, *73*, 330.
19. Karandikar, V. C. *Paintindia* **2006**, *56*, 55.
20. Matyjaszewski, K.; Tsarevsky, N. V. *Nature Chem.* **2009**, *1*, 276.
21. Ramanen, P.; Pitkanen, P.; Jamsa, S.; Maunu, S. L. *J. Polym. Environ.* **2012**, *20*, 950.
22. Dziczkowski, J.; Soucek, M. D. *J. Coat. Technol. Res.* **2010**, *7*, 587.
23. Seniha Güner, F.; Yağcı, Y.; Tuncer Erciyes, A. *Prog. Polym. Sci.* **2006**, *31*, 633.
24. Van Hamersveld, E. M. S.; Van Es, J. J. G. S.; German, A. L.; Cuperus, F. P.; Weissenborn, P.; Hellgren, A. C. *Prog. Org. Coat.* **1999**, *35*, 235.
25. Nasar, A. S.; Subramani, S.; Radhakrishnan, G. *Polym. Int.* **1999**, *48*, 614.
26. Du, H.; Zhao, Y.; Li, Q.; Wang, J.; Kang, M.; Wang, X.; Xiang, H. *J. Appl. Polym. Sci.* **2008**, *110*, 1396.
27. Ranjbar, Z.; Montazeri, S.; Nayini, M.; Jannesari, A. *Prog. Org. Coat.* **2010**, *69*, 426.
28. Lee, S.-Y.; Mohan, D. J.; Kang, I.-A.; Doh, G.-H.; Lee, S.; Han, S. O. *Fiber Polym.* **2009**, *10*, 77.
29. Haque, M. K.; Kawai, K.; Suzuki, T. *Carbohydr. Res.* **2006**, *341*, 1884.
30. Nasirtabrizi, M. H.; Ziaei, Z. M.; Jadid, A. P.; Fatin, L. Z. *Int. J. Ind. Chem.* **2013**, *4*, 11.
31. Ouyang, J.; Xu, Q.; Chu, C.-W.; Yang, Y.; Li, G.; Shinar, J. *Polymer* **2004**, *45*, 8443.
32. Dziczkowski, J.; Dudipala, V.; Soucek, M. D. *Prog. Org. Coat.* **2012**, *73*, 308.